Asian Journal of Chemistry; *Vol. 38, No. 5 (2026), 1196-1206*

ASIAN JOURNAL OF CHEMISTRY

https://doi.org/10.14233/ajchem.2026.35635

Curcumin-Pyrazole Hybrids bearing *bis*(*N*-Arylacetamides): Synthesis, Antiproliferative Activity and Cell Cycle Analysis

NARSAIAH CHELIMELA and SHOBHA RANI SATLA*

Centre for Pharmaceutical Sciences, Jawaharlal Nehru Technological University Hyderabad, Kukatpally, Hyderabad-500085, India

*Corresponding author: E-mail: shobharanisatla123@gmail.com; shobharanisatla@gmail.com

Received: 22 January 2026 *Accepted*: 16 March 2026 *Published online*: 4 May 2026 AJC-22344

In present work, a new series of modified curcumin analogs of *bis*(*N*-arylacetamides) (**6-10**) was synthesised in good yields. The synthesised compounds were characterised by spectral data and the curcumin hybrids **6-10** were evaluated *in vitro* by MTT assay for antiproliferative activity against four different human breast carcinoma cell lines. Compounds **10** and **7** show moderate to better $IC_{50} \pm$ SEM (μM) in the range of 66.52 ± 4.53 to 97.79 ± 3.63 and 71.28 ± 4.30 to 99.18 ± 5.99, respectively against MCF-7, MDA MB-231, MDA MB-436 and MDA MB-453 breast cancerous cell lines. Compounds **10** and **7** have shown a significant inhibition against all the cell lines. Cell cycle analysis of compound **10** in MCF-7 cells revealed a pronounced accumulation of the cell population in the S phase (63.67%), indicating effective S-phase arrest. This suggests that the compound interferes with DNA replication processes. Docking studies with EGFR2 have shown higher glide scores, -5.857 and -5.448 kcal/mol, respectively, for compounds **10** and **7**. The results indicate that the curcumin-pyrazole *bis*(N-arylacetamide) hybrid adducts as a promising lead to develop as antiproliferative agents.

Keywords: Curcumin-pyrazole, Human breast carcinomal cell lines, Antiproliferative, MTT assay, Cell cycle analysis.

INTRODUCTION

Anticancer research has been predominantly focused on natural agents and many of the approved anticancer agents are obtained from natural sources. Most of the natural agents are nontoxic [1-3]. Cancer is an abnormal condition in which uncontrolled proliferation of cells may be observed, due to deregulation of growth promoter and suppressor genes [4]. As per the statistics of Globocon 2022, about 20 million cancer cases and approximately 10 million deaths were recorded; it is expected to reach 35 million by 2050 worldwide. In 2023, 31% of breast cancers alone were noticed in women [5].

Structurally, curcumin is a symmetrical and linear diaryl heptane, contains two substituted phenyl groups. Curcumin is extracted from the rhizomes of the turmeric plant and acts as a bioactive compound. Along with the curcumin, some other curcuminoids are also obtained from turmeric plant extraction [6,7]. Moreover, curcumin is safe even at higher doses and nontoxic. The great advantage of the curcumin scaffold is its involvement in multiple signal transduction mechanisms [8-10]. The extensive research evidenced that curcumin and its derivatives are therapeutically promising agents for various diseases like anti-Alzheimers [11], cardiovascular [12], antidiabetic [13], antioxidant [14], antimicrobial [15], anti-inflammatory [16], wound healing [17], antiviral [18] and anticancerous cells [19-21].

Interestingly, *in vitro* studies with various cancer cell lines evidenced that curcumin showed potentiating effects like the anticancer agents such as doxorubicin, cisplatin and 5-fluorouracil [22]. Some curcumin-based cancer clinical trials also reported including bladder and cervical, colorectal, skin, liver, breast and oral cancers [23-29]. Despite all the aforementioned advantages, curcumin is also facing pharmacokinetic challenges and has some limitations. These limitations are due to various barriers when it is exposed to the biological system like, poor aqueous solubility, metabolic instability, low bioavailability and low cell uptake. To address these limitations, most of the researchers have selected various structural modification strategies. The structural components of curcumin are more flexible to synthesize different curcumin-hybrids. The Michael acceptor region and the two phenolic groups are the major modification centres on curcumin. The formation of curcumin-hybrid heterocycles like pyrazole, imidazole, thiazole and oxazole with a molecular hybridisation approach has already been established. The modified curcumin and its derivatives not only address the pharmacokinetic challenges but also improve the pharmacological activity [19,30,31]. Moreover, many of the cancer cells develop resistance towards anticancer agents through the ATP cassette mechanism. Indeed, noticeable anticancer research is essential to develop potent anticancer agents for the emerging world.

Several pyrazole-containing heterocyclic anticancer agents approved by the Food and Drug Administration (FDA) (Fig. 1) have served as key sources of inspiration [32-35]. Similarly, curcumin has also been reported to exhibit significant cytotoxic activity against a variety of cancer types. Accordingly, the present study proposes the design and synthesis of modified curcumin–pyrazole hybrids as potential antiproliferative agents. It can be achieved by combining two different pharmacophores (curcumin and pyrazole) through a molecular hybridisation strategy and by modifying the two phenolic -OH on the targeted nucleus (Fig. 2).

EXPERIMENTAL

All the chemicals were sourced from Sigma-Aldrich, USA. Reagents used in the entire synthesis process were commercially obtained from the other chemical suppliers. Analytical grade solvents were preferred without any further purification. MDL Accelrys® 4.1. Version software was employed to determine the IUPAC nomenclature for the obtained compounds. The progress of the reaction was monitored by thin-layer chromatography (TLC), visualised under UV light. Aluminum precoated plates of silica gel Kieselgel 60 F_{254} from Merck with 0.2 mm thickness are preferred. The synthesized compounds were characterized by ^{1}H NMR and LC-MS techniques. ^{1}H

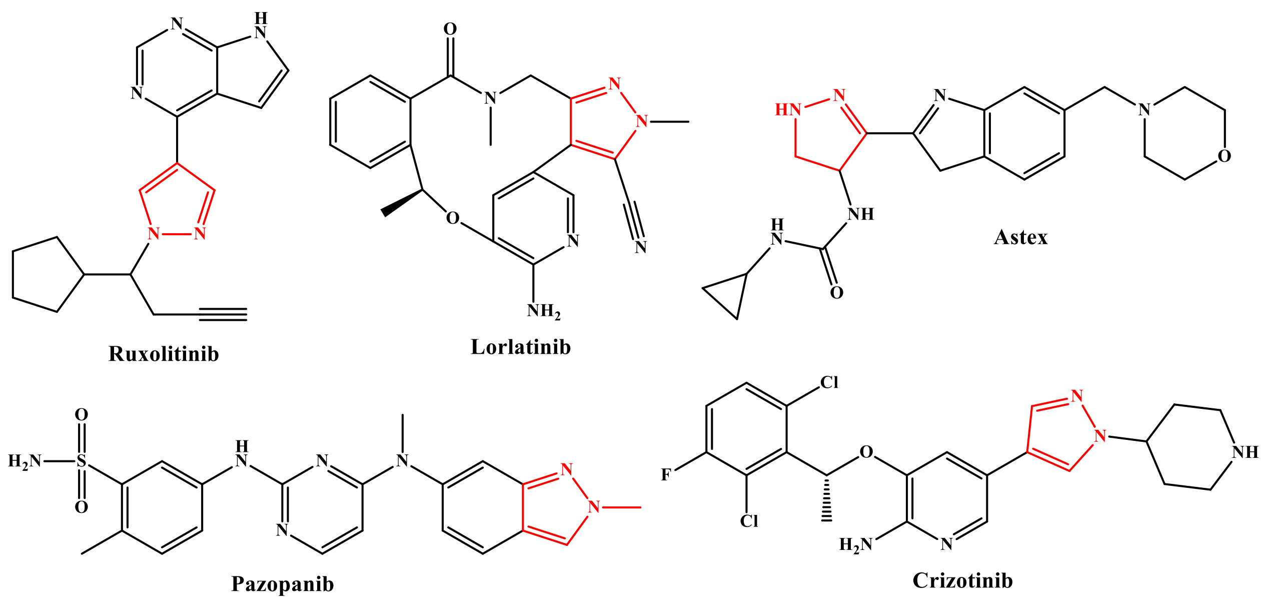

Fig. 1. Chemical structures of pyrazole containing FDA-approved anticancer agents

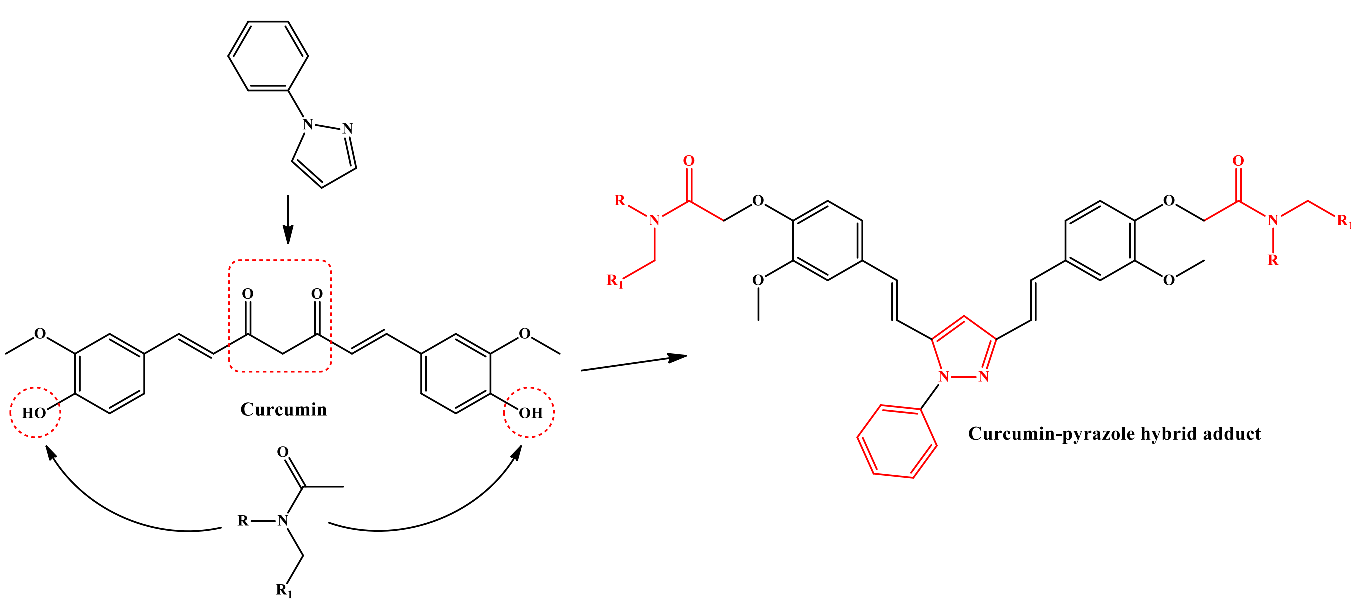

Fig. 2. Proposed modifications to curcumin

NMR spectra were recorded on a Bruker 400 MHz spectrometer using $CDCl_3$ as solvent and TMS as the internal standard; chemical shifts (δ) are reported in ppm and coupling constants (*J*) in Hz. LC-MS analyses were performed on an Agilent Technologies HPLC system equipped with an electrospray ionization source operating in positive mode.

Synthesis: Compound **3** (curcumin) was synthesized from vanillin and acetylacetone according to literature procedures [36].

General procedure for the synthesis of 4,4′-((1*E*,1′*E*)-(1-phenyl-1*H*-pyrazole-3,5-diyl)*bis*(ethene-2,1-diyl))*bis*(2-methoxyphenol) (5): Curcumin (**3**) (5.0 g, 15.5 mmol) and phenyl hydrazine (**4**) (2.93 g, 27.1 mmol) were suspended in acetic acid (50 mL) and the heterogeneous reaction mass was stirred at 70 ºC for 2 h. TLC analysis indicated complete consumption of both reactants; the reaction mixture was cooled to room temperature and then diluted with water (50 mL, 10 vol). The precipitated solid was filtered and washed with 100 mL of water. The obtained brown solid was dried at 50 ºC for 2 h under vacuum and purified by column chromatography on 60-120 grade silica gel and (40:60 ethyl acetate, hexane) yielded 5.2 g (87.1%) of pure product **5** as a light brown solid [36].

General procedure for the synthesis of compounds 6-10: To a solution of 4,4′-((1*E*,1′*E*)-(1-phenyl-1*H*-pyrazole-3,5-diyl)-*bis*(ethene-2,1-diyl))*bis*(2-methoxyphenol) (**5**) (300 mg, 0.68 mmol) in DMF was added corresponding chloroacetamide (1.5 mmol; **6a-10a**) and potassium carbonate (282 mg, 2.04 mmol) at room temperature then refluxed for 12 h. After completion of the reaction cooled to room temperature and water was added, the resultant gummy reaction mass was extracted with Dichloromethane the organic layer was washed with water, dried over sodium sulphate, distilled out at reduced pressure and purified on 60-120 mesh silica gel eluted with EtOAc: hexane 40:60 to give pure product **6-10** as solid (**Scheme-I**).

2,2′-((((1*E*,1′*E*)-(1-Phenyl-1*H*-pyrazole-3,5-diyl)*bis*-(ethene-2,1-diyl))*bis*(2-methoxy-4,1-phenylene))*bis*(oxy))-*bis*(*N*-benzylacetamide) (6): Yield: 76%; m.p.: 185-189 ºC, ^{1}H NMR (400 MHz, $CDCl_3$, δ ppm): 7.53 (s, 2H, NH), 7.52-7.38 (m, 5H, Ar-H), 7.35-7.21 (m, 10H, Ar-H), 7.16-6.99 (m, 8H, Ar-H, -C=CH), 6.92 (s, 1H, py-CH), 6.85 (s, 1H, Ar-H), 6.78 (d, 1H, *J* = 16 Hz, -C=CH), 4.53 (s, 4H, $-OCH_2$), 4.61 (s, 4H, $-NCH_2$), 3.71 (s, 3H, $-OCH_3$), 3.69 (s, 3H, $-OCH_3$); ^{13}C NMR (400 MHz, $CDCl_3$, δ ppm): 168.52, 151.02, 149.80, 147.48, 139.35, 137.71, 131.74, 129.27, 128.02, 127.55, 125.25, 120.14, 115.86, 114.76, 109.85, 108.97, 55.46, 43.06; LC-MS (ESI) *m/z*: $(M+H)^+$ calcd. ($C_{45}H_{42}N_4O_6$+H) 735.85, found 735.2, RT = 6.268 min.

2,2′-((((1*E*,1′*E*)-(1-Phenyl-1*H*-pyrazole-3,5-diyl)*bis*-(ethene-2,1-diyl))*bis*(2-methoxy-4,1-phenylene))*bis*(oxy))-*bis*(*N*-benzyl-*N*-methylacetamide) (7): Yield: 86%; m.p.: 172-175 ºC; ^{1}H NMR (400 MHz, $CDCl_3$, δ ppm): 7.53-7.41 (m, 5H, Ar-H), 7.34-7.21 (m, 10H, Ar-H), 7.16-6.99 (m, 8H, Ar-H, -C=CH), 6.92 (s, 1H, py-CH), 6.85 (s, 1H, Ar-H), 6.78 (d, 1H, *J* = 16 Hz, -C=CH), 4.53 (s, 4H, $-OCH_2$), 4.61 (s, 4H, $-NCH_2$), 3.71 (s, 3H, $-OCH_3$), 3.69 (s, 3H, $-OCH_3$), 3.01 (s, 3H, $-NCH_3$), 3.00 (s, 3H, $-NCH_3$); ^{13}C NMR (400 MHz, $CDCl_3$, δ ppm): 168.11, 167.62, 151.11, 149.57, 147.10, 142.30, 139.36, 136.07, 131.45, 130.12, 129.10, 128.46, 127.35, 126.55, 125.08, 119.72, 114.02, 109.04, 55.51, 51.06. MS (ESI) *m/z*: $(M+H)^+$ calcd. ($C_{47}H_{46}N_4O_6$+H) 763.91, found 763.15.

2,2′-((((1*E*,1′*E*)-(1-Phenyl-1*H*-pyrazole-3,5-diyl)*bis*-(ethene-2,1-diyl))*bis*(2-methoxy-4,1-phenylene))*bis*(oxy))-*bis*(*N*-phenylacetamide) (8): Yield: 84%; m.p.: 166-169 ºC, ^{1}H NMR (400 MHz, $CDCl_3$, δ ppm): 8.88-8.82 (s, 2H, NH), 7.52-7.38 (m, 5H, Ar-H), 7.35-7.21 (m, 10H, Ar-H), 7.16-6.99

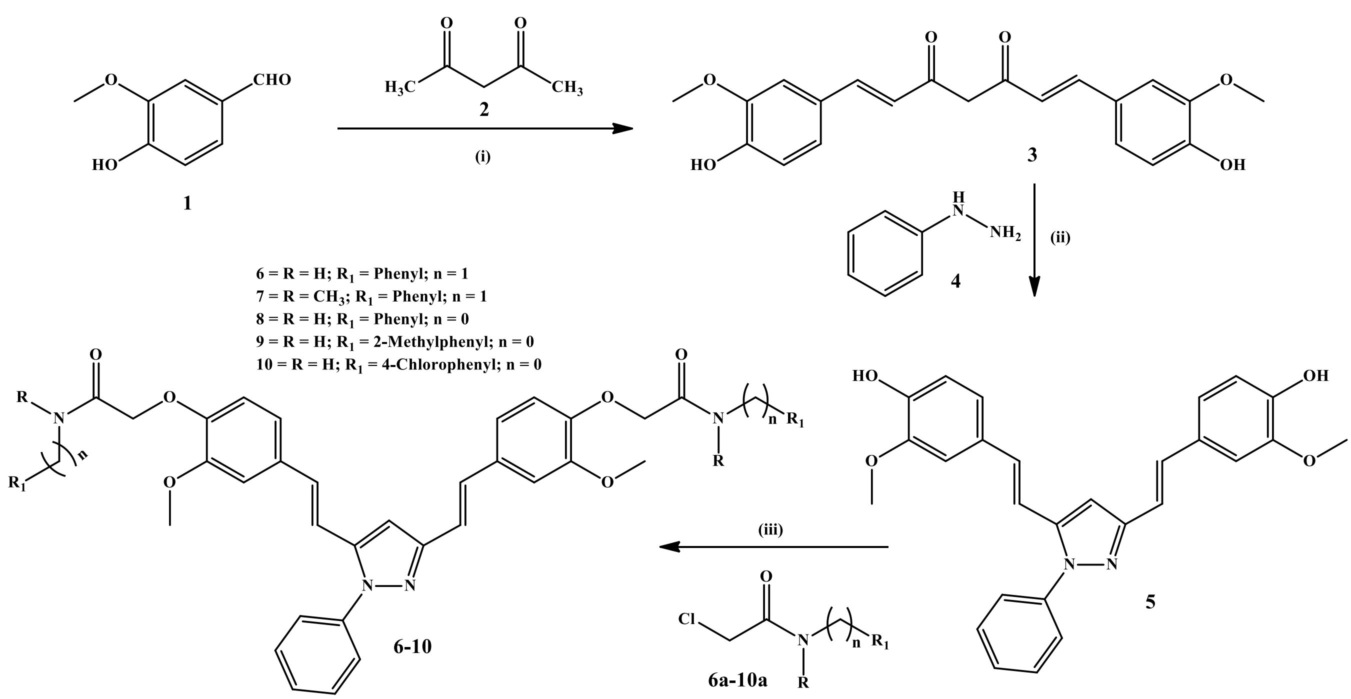

Scheme-I: Reagents and conditions: (i) $B(OnBu)_3$, EtOAc, butylamine, reflux, (ii) acetic acid, stirring at 68-70 ºC for 2 h, 80-82%, (iii) Corresponding N-substituted chloroacetamides, DMF, K_2CO_3, at 80 ºC, reflux for 12 h, 70-91%

(m, 8H, Ar-H, -C=CH), 6.92 (s, 1H, py-CH), 6.85 (s, 1H, Ar-H), 6.78 (d, 1H, J = 16 Hz, -C=CH), 4.53 (s, 4H, -OCH_2), 3.71 (s, 3H, -OCH_3), 3.69 (s, 3H, -OCH_3); ^{13}C NMR (400 MHz, $CDCl_3$, δ ppm): 166.72, 151.00, 149.91, 147.00, 139.37, 137.08, 132.07, 131.63, 129.04, 128.00, 125.22, 124.62, 120.04, 119.86, 116.27, 114.96, 110.06, 109.23, 55.86; MS (ESI) *m/z*: $(M+H)^+$ calcd. ($C_{43}H_{438}N_4O_6$+H) 707.80, found 707.01.

2,2′-((((1*E*,1′*E*)-(1-Phenyl-1*H*-pyrazole-3,5-diyl)*bis*-(ethene-2,1-diyl))*bis*(2-methoxy-4,1-phenylene))*bis*(oxy))-*bis*(*N*-(*o*-tolyl)acetamide) (9): Yield: 87%; m.p.: 171-173 ºC, ^{1}H NMR (400 MHz, $CDCl_3$, δ ppm): 8.69 - 8.01 (s, 2H, NH), 7.52-7.38 (m, 5H, Ar-H), 7.35-7.21 (m, 8H, Ar-H), 7.16-6.99 (m, 8H, Ar-H, -C=CH), 6.92 (s, 1H, py-CH), 6.85 (s, 1H, Ar-H), 6.78 (d, 1H, J = 16 Hz, -C=CH), 4.53 (s, 4H, -OCH_2), 3.71 (s, 3H, -OCH_3), 3.69 (s, 3H, -OCH_3), 2.31 (s, 3H, -$ArCH_3$), 2.30 (s, 3H, -$ArCH_3$); ^{13}C NMR (400 MHz, $CDCl_3$, δ ppm): 166.26, 151.01, 149.61, 147.01, 139.36, 135.04, 134.99, 132.29, 131.52, 129.20, 128.21, 127.93, 126.78, 125.02, 121.90, 119.57, 109.74, 108.90, 55.61; MS (ESI) *m/z*: $(M+H)^+$ calcd. ($C_{45}H_{42}N_4O_6$+H) 735.85, found 735.01.

2,2′-((((1*E*,1′*E*)-(1-Phenyl-1*H*-pyrazole-3,5-diyl)*bis*-(ethene-2,1-diyl))*bis*(2-methoxy-4,1-phenylene))*bis*(oxy))-*bis*(*N*-(4-chlorophenyl)acetamide) (10): Yield 90%; m.p.: 192-195 ºC, ^{1}H NMR (400 MHz, $CDCl_3$, δ ppm): 8.92-8.86 (s, 2H, NH), 7.52-7.38 (m, 5H, Ar-H), 7.35-7.21 (m, 8H, Ar-H), 7.16-6.99 (m, 8H, Ar-H, -C=CH), 6.92 (s, 1H, py-CH), 6.85 (s, 1H, Ar-H), 6.78 (d, 1H, J = 16 Hz, -C=CH), 4.53 (s, 4H, -OCH_2), 3.71 (s, 3H, -OCH_3), 3.69 (s, 3H, -OCH_3); ^{13}C NMR (400 MHz, $CDCl_3$, δ ppm): 166.79, 150.97, 149.92, 147.33, 139.37, 135.70, 133.01, 132.22, 131.58, 129.77, 128.05, 125.23, 121.02, 119.95, 116.45, 109.27, 109.74, 55.91; MS (ESI) *m/z*: $(M+H)^+$ calcd. ($C_{43}H_{36}Cl_2N_4O_6$+H) 776.68, found 778.19.

Pharmacological assay

Evaluation of antiproliferative activity using MTT assay and IC_{50} calculations: An MTT (3-[4,5-dimethylthiazol-2-yl]-2,5-diphenyltetrazolium bromide) assay was aimed to determine the antiproliferative activity of all the synthesised compounds against four different human breast cancer cell lines, MCF7, MDA-MB-231, MDA-MB-453 and MDA-MB-436. The cancer cell lines were sourced from NCCS, Pune. Initially, primary concentrations (18, 6, 2, 0.666, 0.222, 0.074, 0.025 mM) of test compounds **6-10** were prepared in DMSO from the primary stocks. MTT (5 mg/mL) primary stock solution was prepared in phosphate buffer saline (PBS). The stocks are preserved at 20 ºC until further use. Cells were removed from the culture flask containing growth medium. A 5 mL of PBS was used to wash the cells. After removing the PBS, 1 mL of Trypsin EDA was added and placed at 37 ºC for 5 min in the CO_2 incubator. After detachment, the cells were collected into a sterile centrifuge tube and centrifuged for 5 min at 1500 rpm. Cells were further seeded in 96-well plates at a density of 5000cells/well and incubated at 37 ºC overnight in a CO_2 incubator. After, the culture medium was removed and 100 μL fresh culture medium was added to respective wells containing test compound at different final concentrations (180, 60, 20, 6.67, 2.22, 0.74, 0.25 μM) in triplicate and incubated for 48 h in a CO_2 incubator. After incubation, MTT reagent was added at a final concentration of 0.5 mg/mL and incubated for the formation of formazan crystals. The formed crystals were dissolved in DMSO to read the optical density at 570 nm on the SpectraMax M4 ELISA microplate reader. Cell viability percentage was calculated by using the following formula:

$$\text{Cell viability (\%)} = \frac{OD_{570}\ \text{treatment}}{OD_{570}\ \text{control}} \times 100$$

Further IC_{50} values were calculated, using GraphPad Prism software, applying nonlinear regression analysis by following the equation: -log (inhibitor) *vs.* response-variable slope (Four parameter).

Cell cycle analysis: Human breast cancer (MCF-7) cells (1×10^5 cells/well) were seeded in 6-well plates. After 24 h, the medium was removed and replaced by fresh culture medium containing optimised concentrations (half of the IC_{50} concentration) of active compound **10**. The cell cycle pattern was analysed by measuring the amount of propidium iodide (PI)-labeled DNA in ethanol-fixed cells. In brief, the cells were exposed to the stimuli for 48 h, harvested by trypsinisation and fixed with chilled 70% ethanol. Cells will be stained for total DNA content with PI (1 mg/mL) staining buffer containing RNase enzyme according to the manufacturer's instructions. The cell cycle analysis was performed to determine their percentages of cells in different phases like G0-G1, S and G2/M, under different treatments. The percentages of cells in different phases in the sample were analysed using a flow cytometer (Becton Dickinson, San Jose, USA) and ModFit software.

Statistical statement: Cell cycle distribution was analysed by flow cytometry following PI staining. Data were obtained from three independent experiments (n = 3) and expressed as mean ± standard deviation (SD). Statistical analysis was performed using one-way ANOVA followed by Tukey's post hoc test. Differences were considered statistically significant at $p < 0.05$.

Molecular docking studies: Ligand structure drawing, 3D conversion and initial energy minimisation were performed utilizing the pcm10 tool (Serena Software, Bloomington, USA). The Ligprep tool of Schrödinger was used for the preparation of the ligands. All protein structures were accessed from the PDB database. In the execution of molecular docking analysis studies, the Glide tool of Schrödinger was used. The Desmond module (D.E. Shaw Research, New York, USA) was employed for performing the molecular dynamics simulations and subsequent analysis.

The target genes/protein prediction was performed by using the binding DB online server and Swiss Target Prediction for the representative designed molecules [37,38]. After the comparative analysis of the scores and ratio data of the two servers, potential anticancer targets like Endothelial Growth Factor Receptor (EGFR2) (3w2r) were selected as target proteins for docking. 3D structures of selected targets were accessed from the PDB database. Using the Glide program of Maestro, a grid box of 16 Å × 16 Å × 16 Å was made around the selected binding cavity of the protein 3w2r. The possible interactions and affinities of the compounds were determined using flexible docking in the Glide program. Using the extra precision (XP) docking tool, molecular docking was performed, keeping all the parameters set to default values [39].

RESULTS AND DISCUSSION

All the proposed analogues of modified curcumin–pyrazole derivatives (**6-10**) were synthesized *via* a multi-step protocol employing a molecular hybridization strategy. In the first step, curcumin (**3**) was obtained by the condensation of vanillin (**1**) and acetylacetone (**2**) in the presence of tributoxyborane, dry ethylacetate and *n*-butylamine. In the next step, substituted pyrazole-curcumin (**5**) was obtained by the replacement of the diketone moiety by treating curcumin with phenyl hydrazine (**4**) in the presence of acetic acid. The synthesis of compounds **3** and **5** has been previously reported, and the present work followed the established literature procedures [36]. The key intermediate **5** was used to get the desired target compounds **6-10**, by treating with corresponding substituted *N*-aryl chloroacetamides (**6a-10a**). The desired final compounds were obtained in the presence of potassium carbonate at reflux at 80 ºC for 12 h in DMF. All the synthesised compounds were purified by column chromatography using 60-120 silica gel eluting with ethyl acetate and hexane. Further, the target compounds **6-10** were characterised and confirmed by ^{1}H NMR, ^{13}C NMR and mass spectral data. Proton NMR spectra of compounds **6-10** showed the appearance of a singlet corresponding to the pyrazole -CH proton at δ 6.92 ppm and the vinylic protons emerged at δ 6.78 ppm as a doublet with a *J* value of 16.0 Hz. Another singlet appeared in the range of δ 3.81-3.89, corresponding to -CH_2 protons. Two sets of methoxy protons as singlets were appeared in the range of δ 3.71-3.69 ppm. The -NH proton appeared as a singlet at δ 8.92-7.53 ppm and the -NCH_2 protons were observed at δ 4.61 ppm as a singlet.

Antiproliferative activity

***In vitro* cytotoxic evaluation:** *In vitro* cytotoxic activity of curcumin-pyrazole derivatives **6-10** was determined by using MTT assay against cell growth of four different human breast carcinoma cell lines (MCF-7, MDA-MB-231, MDA-MB-436, MDA-MB-453). All the cell lines are treated with different concentrations of test compounds (180, 60, 20, 6,67, 2.22, 0.74, 0.25 μM) and curcumin and doxorubicin (Dox) were used as a reference and positive control, respectively. The evaluated IC_{50} values (Table-1) indicate that the electronic effects of the substitution pattern with different bioisosters on the curcumin-pyrazole hybrid greatly influence the proliferative activity. All the test compounds have gained mild to moderate activity compared with curcumin and doxorubicin. Compounds **10**, **7** and **9** have shown comparatively better cytotoxic activity, whereas compounds **8** and **6** exhibited moderate cytotoxic activity against all the cell lines.

MTT assay results demonstrated that compounds **6-10** exhibited superior activity against the MCF-7 and MDA-MB-453 cell lines compared to the other evaluated cell lines. Compound **10**, curcumin-pyrazole acetamide derivative with a 4-chlorophenyl substitution, has shown a very less percentage of cell viability (Fig. 3) compared with other derivatives and the IC_{50} values are in the range of 66.52 ± 4.53 to 97.79 ± 3.63 μM against the cell lines. Compound **7**, having an unsubstituted phenyl ring and an additional N-CH_3 substitution, is the next best molecule with IC_{50} values in the range of 71.28 ± 4.30 to 99.18 ± 5.99 μM. Compound **9** is a methoxyphenyl derivative, showing better activity against all the cell lines, with IC_{50} values in the range of 76.34 ± 4.61 to 99.77 ± 6.02 μM. Compound **8** is an unsubstituted phenyl ring and the absence of a methylene bridge between nitrogen and the phenyl ring containing derivative, which shows moderate cytotoxic activity against all the cell lines, with IC_{50} values in the range of 84.18 ± 5.08 to 104.04 ± 6.28 μM. Compound **6** is an unsubstituted phenyl ring and having a methylene bridge between the nitrogen atom and the phenyl ring containing derivative, it shows very little cytotoxic activity in the series with IC_{50} values in the range of 93.24 ± 5.63 to 102.18 ± 6.17 μM.

The structure activity relationship (SAR) analysis of compounds **6-10** (Fig. 4) indicates that all the compounds have common structural aspects. The pyrazole-curcumn scaffold is essential for cytotoxic activity and improves the stability of the compound. The results indicate that the introduction of the pyrazole moiety in place of the diketo of curcumin not only improves the activity but also improves the pharmacokinetic profile of the synthesised compound. Modification of phenolic groups by various substituted acetamides greatly increases the solubility pattern of the modified curcumin. The electronic and hydrophobic properties are also altered when it is a hybrid than the curcumin alone. All the test compounds **6-10** exhibited better to moderate cytotoxicity based on the groups present on the phenyl ring, the number of carbon atoms between the amide nitrogen atom to phenyl and the presence/absence of substitution on the amide nitrogen atom. The presence of either a 2º or 3º nitrogen atom is essential to enhance the cytotoxic activity. The electron-withdrawing groups present on the phenyl ring (compound **10**; 4-chlorophenyl) increase the activity than electron-donating groups (compound **9**; 2-methoxyphenyl). Compound **7**, featuring a tertiary nitrogen

TABLE-1
ANTIPROLIFERATIVE ACTIVITY DATA AGAINST HUMAN BREAST CARCINOMA CELL LINES OF COMPOUNDS **6-10**

Compound	IC_{50} ± SEM (μM)			
	MCF-7	MDA MB-231	MDA MB-436	MDA MB-453
6	96.29 ± 5.81	102.18 ± 6.17	101.63 ± 6.13	93.24 ± 5.63
7	76.14 ± 4.59	94.62 ± 5.71	99.18 ± 5.99	71.28 ± 4.30
8	84.18 ± 5.08	97.17 ± 5.86	104.04 ± 6.28	87.21 ± 5.26
9	79.18 ± 4.78	95.99 ± 5.79	99.77 ± 6.02	76.34 ± 4.61
10	71.57 ± 4.32	90.73 ± 5.90	97.79 ± 3.63	66.52 ± 4.53
Curcumin	61.92 ± 3.09	49.56 ± 2.47	73.90 ± 3.69	70.32 ± 3.51
Dox	15.22 ± 0.76	0.154 ± 0.00	30.96 ± 1.54	22.42 ± 1.12

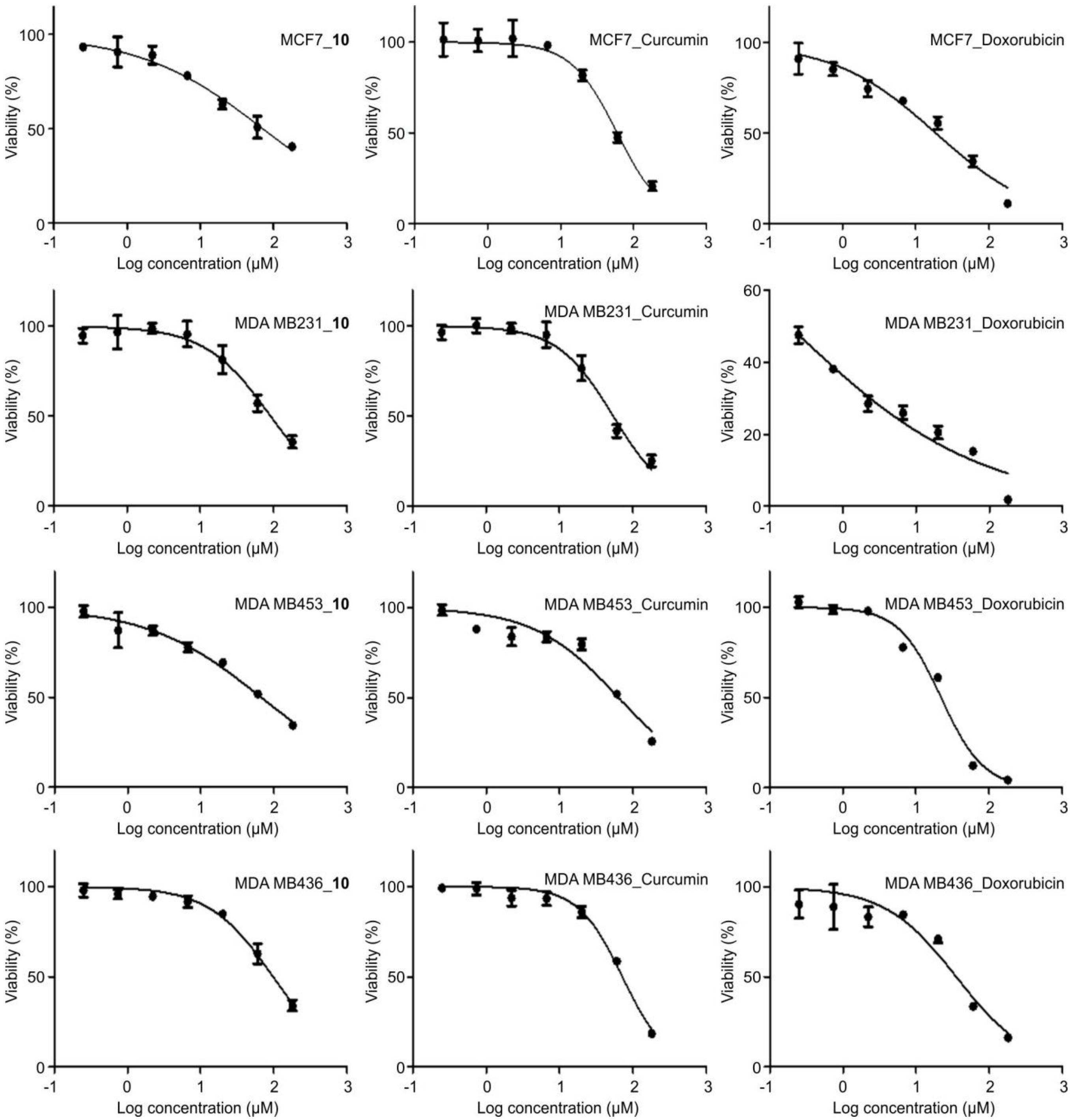

Fig. 3. % Cell viability of compound **10** against MCF-7 cell line, MDA-MB-231 cell line, MDA-MB-453 cell line and MDA-MB-436 cell line

atom positioned one carbon away from the phenyl ring, exhibited greater activity compared to compounds **9**, **6** and **8**.

Cell cycle analysis by flow cytometry: Compound **10** was tested on the MCF-7 cell line for cell cycle distribution. Untreated MCF-7 cells were used as a reference control. Control was used for taking baseline and distribution cells in different phases (G0/G1, S and G2/M). Normal cell proliferation was observed in control cells and the proliferation distribution in different phases was found to be 40.41%, 44.56% and 15.02% in G0/G1, S and G2/M phases, respectively. Curcumin-treated cells have shown a significant increase in the population of G2/M to 34.00% to that of control (15.02%). S-phase cells were decreased to 23.71% from the control, which indicates arrest of G2/M phase (Table-2). Compound **10** treated cells significantly follow a different pattern than control and curcumin, with a predominant increase in the accumulation of cells in S phase by 63.67% and a decrease in other phases by 29.53% (G0/G1) and 6.80% (G2/M). Compound **10** significantly increased the S-phase population to 63.67 ± 3.1% compared to control (44.56 ±

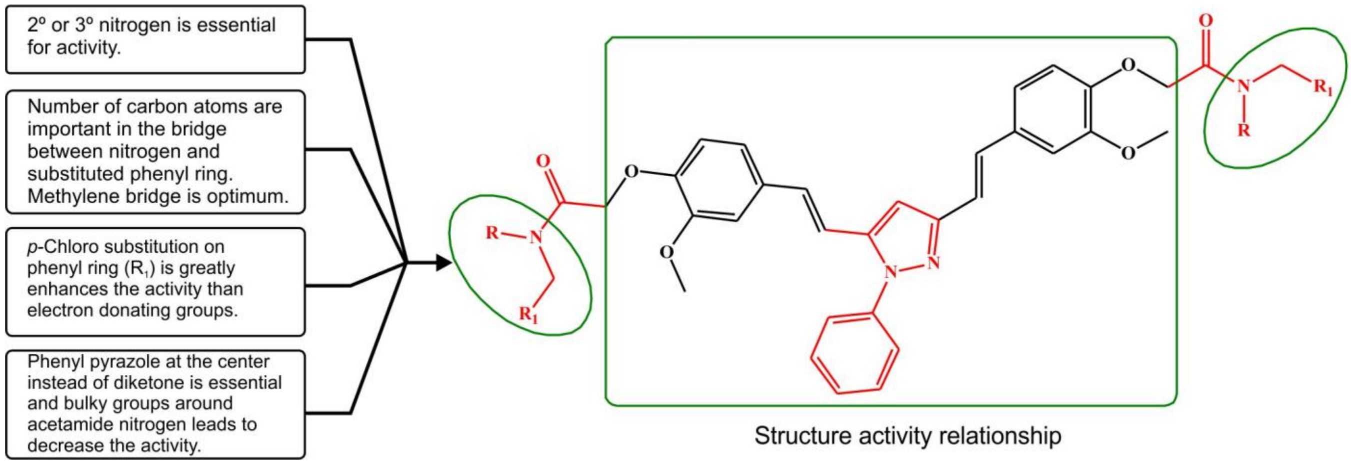

Fig. 4. Structure-activity relationship of compounds **6-10**

TABLE-2
CELL CYCLE DISTRIBUTION (% OF CELLS IN EACH PHASE) AND POSSIBLE MECHANISMS

Treatment	G0/G1(%)	S (%)	G2/M (%)	*p*-value (*vs.* control)
Control	40.41 ± 2.3	44.56 ± 1.8	15.02 ± 1.2	–
Curcumin	42.29 ± 1.9	23.71 ± 2.1	34.00 ± 2.5	$p < 0.01$
Compound **10**	29.53 ± 2.0	63.67 ± 3.1	6.80 ± 1.4	$p < 0.01$

Data are expressed as mean ± SD (n = 3). Statistical analysis was performed using one-way ANOVA followed by Tukey's post hoc test. Differences were considered significant at $p < 0.05$.

1.8%, $p < 0.001$), indicating statistically significant S-phase arrest. Compound **10** induces S-phase accumulation, suggesting possible interference with DNA replication, rather than confirming replication inhibition. Future studies including DNA synthesis assays and replication stress markers are planned to further elucidate the mechanism. In Fig. 5, presented flow cytometry profile in histograms and scattered plots of cell cycle analysis on MCF-7 cells is presented.

Molecular docking: Molecular modeling experiments have revealed the importance of amino acid residues of wild protein taget (EGFR2) like Lys745, Leu 788, Ile 789, Met790 and Met793, which are crucially involved in the ATP site of the enzyme. It is composed of a hydrophobic binding pocket with Leu 747, Ile 759, Met 766, Leu 777 and Leu 788. Another structural element, the DFG motif, is composed of Asp855, Phe856 and Gly857. The urea moiety of the co-crystallised ligand showed hydrogen-bonding interactions with Ala722 and Asp837. The pyrrolo-pyrimidine part of the structure formed hydrogen bonds with Asp855 and Phe856. A π-cation interaction was observed with Arg841. It showed an XP-G score of -10.764.

Compounds from **6-10** show XP G-scores higher than or equal to -4 as shown in Table-3. Compound **10** shows the best glide score of -5.857, with three hydrogen bonding interactions

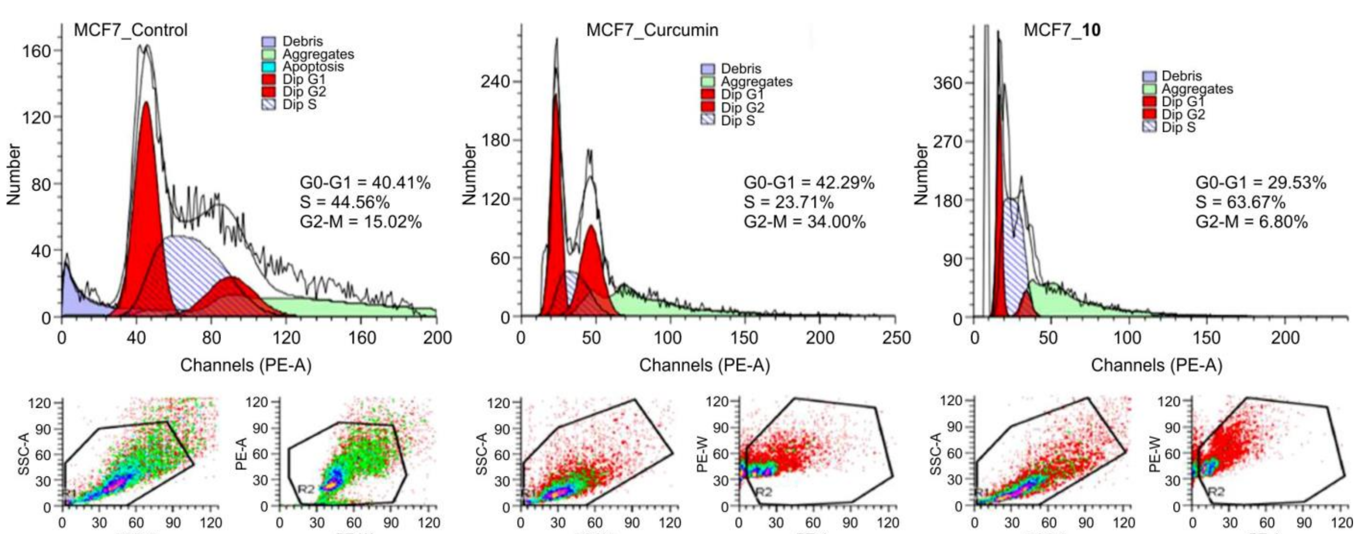

Fig. 5. Flow cytometry histograms and scattered plots of control, curcumin and compound **10**. Data represent mean ± SD of three independent experiments. *$p < 0.05$ *vs.* control

TABLE-3
DOCKING XP G-SCORES AND BINDING INTERACTIONS WITH COMPOUNDS **6-10**

Compound	Glide score	Hydrogen binding interaction with amino acid residues (bond distance in Å)	Other binding interactions (bond distance Å)
6	-4.983	Leu718 (2.91); Val717 (1.01); Val717 (1.03); Cys797 (2.03); Val876 (2.41)	–
7	-5.448	Arg841 (1.96); Arg841 (2.12)	–
8	-4.448	Val876 (2.81)	–
9	-5.152	Ser720 (2.31); Leu718 (2.56); Cys797 (2.21); Arg 841 (2.01)	–
10	-5.857	Leu718 (2.15); Cys797 (2.20); Asp837 (1.83)	pi-pi stacking - Arg841 (3.41); halogen bond - Met793 (1.93)
Curcumin	-8.261	Thr854 (1.97)	pi-pi stacking-Phe856 (3.73)
Cocrystal	-10.764	Gly857 (1.85); Thr854 (2.01); Asp800 (1.96); Cys797 (2.22); Met793 (1.78); Lys745 (1.97)	halogen bond-Leu788 (3.73); pi-pi stacking-Phe856 (3.30)

observed with Leu718 (2.15), Cys797 (2.20) and Asp-837 (1.83) and a π-π stacking interaction with Arg841 (3.41 Å) and a halogen bond with Met793 (1.93 Å). The second highest glide (-5.448) score was observed for compound **7**, with two hydrogen bonding interactions with Arg841 (1.96 Å) and Arg841 (2.12 Å). Compound **9** is the third-ranked molecule and the glide score is about -5.152, with four hydrogen bonding interactions with Ser720 (2.31 Å), Leu718 (2.56 Å), Cys797 (2.21 Å) and Arg 841 (2.01 Å). Compound **6** has shown a moderate glide score (-4.983) with five hydrogen bonding interactions with Leu718 (2.91 Å), Val717 (1.01 Å), Val717 (1.03 Å), Cys797 (2.03 Å) and Val876 (2.41 Å). The least glide score was obtained for compound **8** is about -4.448, with only one hydrogen bonding interaction with Val876 (2.81 Å). The 2D and 3D bonding interactions of compounds **6-10**, co-crystallised ligand and curcumin are shown in Fig. 6.

Docking studies show that the compounds **6-10** showed a stable binding conformation with an active site pocket of the EGFR2 target. The ligands were stabilised *via* hydrogen bonds, hydrophobic bonds and halogen bonds. These types of binding interactions support that the test compounds may significantly interfere with the function of the target proteins.

Conclusion

In current study, designed and synthesised a series of antiproliferative curcumin-pyrazole arylacetamide analogs in good yields. MTT assay of the test compounds on four breast cancer

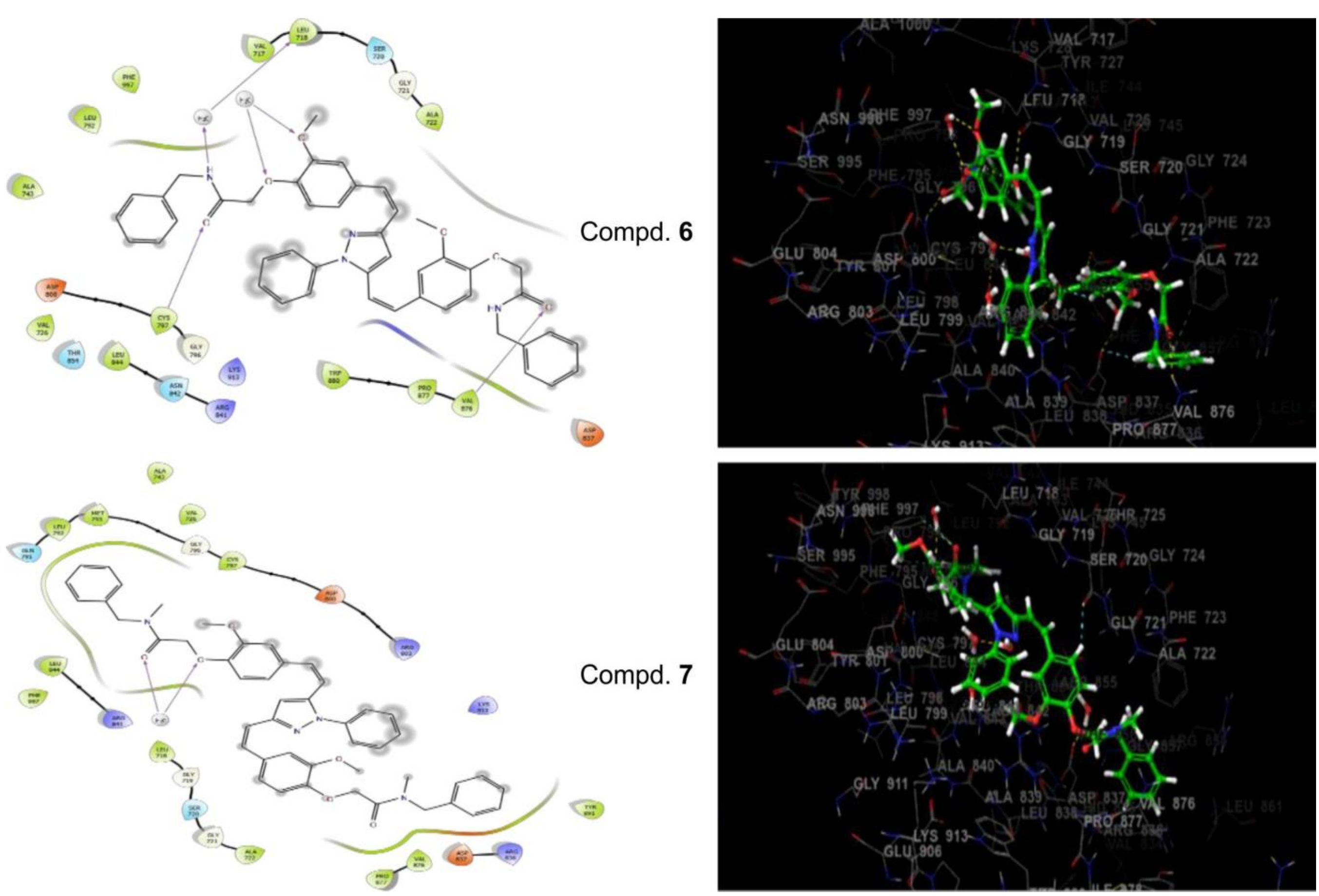

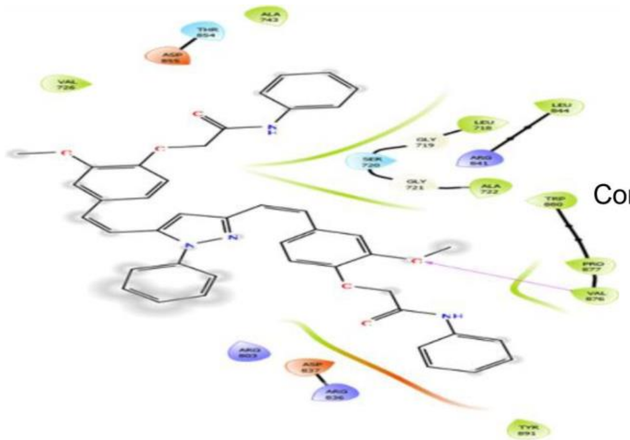

Compd. **8**

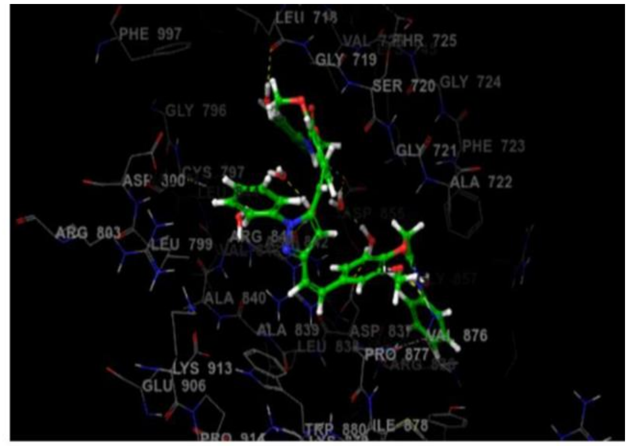

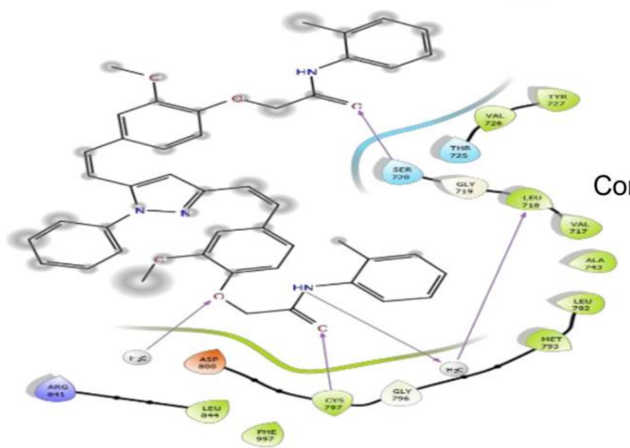

Compd. **9**

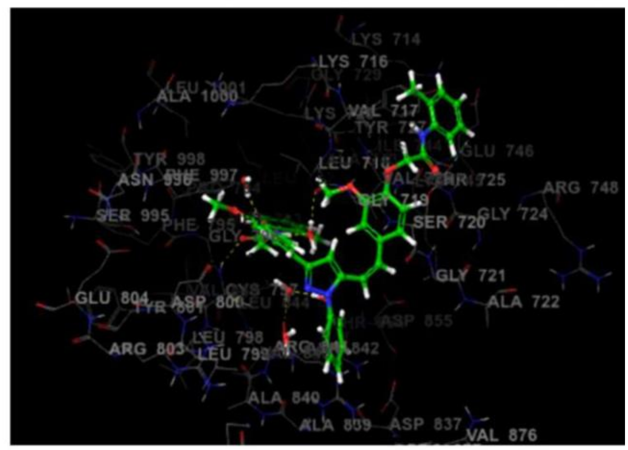

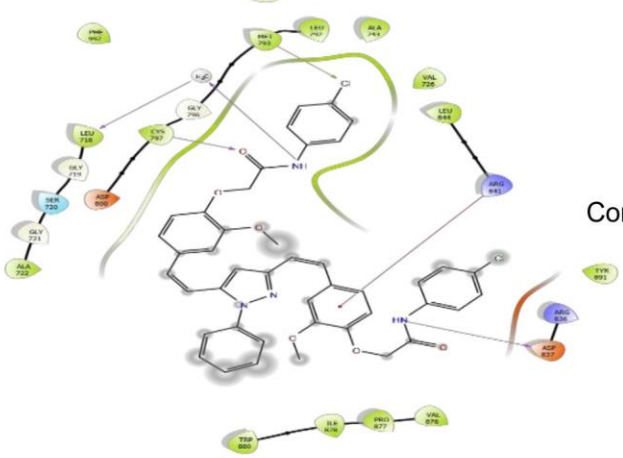

Compd. **10**

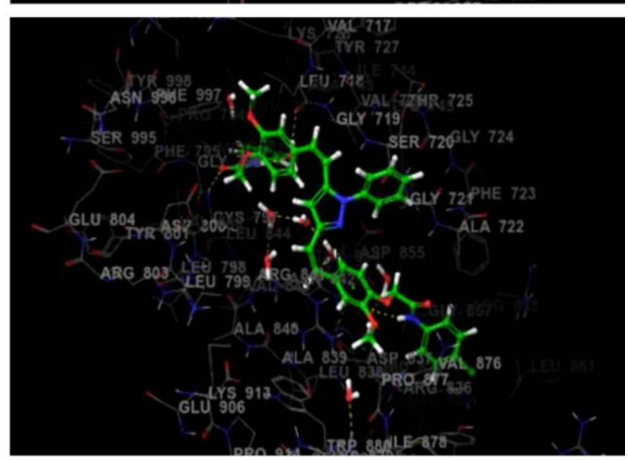

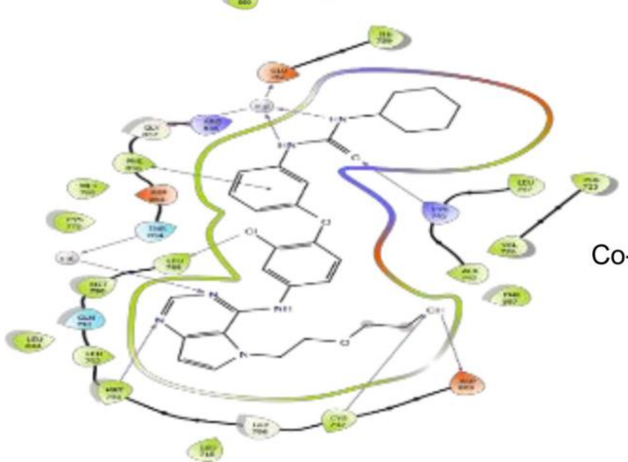

Co-crystal

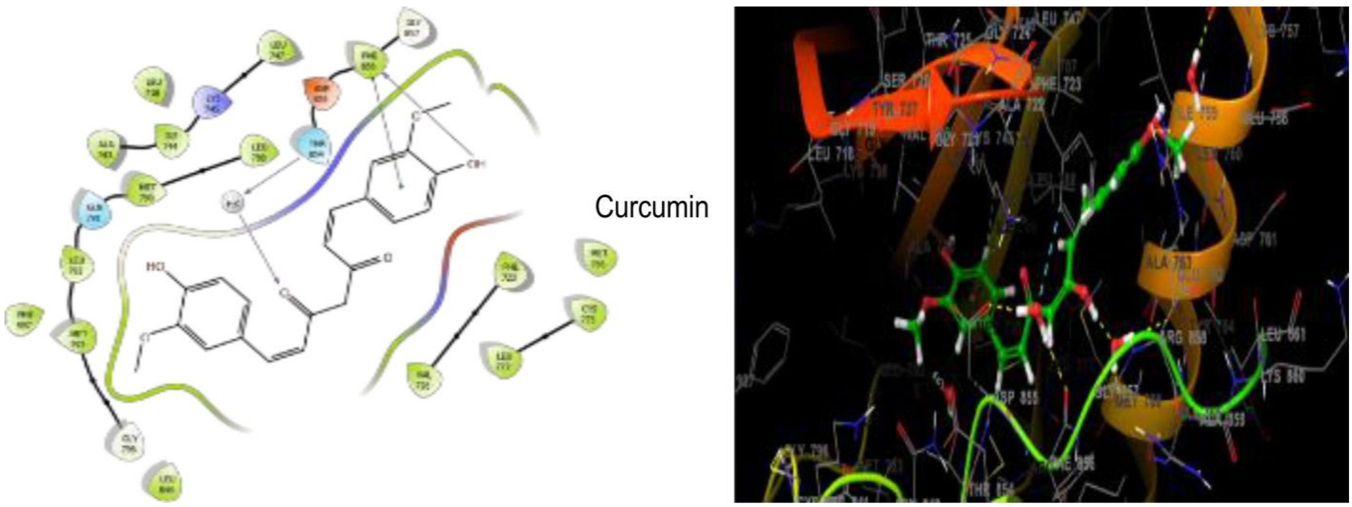

Fig. 6. 2D and 3D bonding interactions of compounds **6-10**, co-crystallised ligand and curcumin

cancer cell lines demonstrated that all the synthesised curcumin-pyrazole based acetamides showed moderate to better anti-proliferative activity. The 4-chloro derivative **10** and unsubstituted **7** showed the best cytotoxicity against all the cell lines. Cell cycle studies on the MCF-7 cell line indicate that the growth of cells was inhibited by arresting the cell cycle in S phase. Molecular docking results suggested that the compounds have moderate to good binding score (glide scores) in the range of -5.857 to -4.448 kcal/mol. Most of the compounds have hydrogen bonds, π-π stacking, hydrophobic and π-cation interactions. These results provide valuable insight into the development of curcumin–pyrazole-based acetamide derivatives as promising candidates for anticancer drug discovery.

CONFLICT OF INTEREST

The authors declare that there is no conflict of interests regarding the publication of this article.

DECLARATION OF AI-ASSISTED TECHNOLOGIES

During the preparation of this manuscript, the authors used an AI-assisted tool(s) to improve the language. The authors reviewed and edited the content and take full responsibility for the published work.

REFERENCES

1. C. Chen, Y. Feng, C. Zhou, Z. Liu, Z. Tang, Y. Zhang, T. Li, C. Gu and J. Chen, *Bioorg. Chem.*, **153**, 107772 (2024); https://doi.org/10.1016/j.bioorg.2024.107772
2. P. Quintero-Rincón, K. Caballero-Gallardo and J. Olivero-Verbel, *Nat. Prod. Bioprospect.*, **15**, 25 (2025); https://doi.org/10.1007/s13659-025-00511-0
3. Y. Yang, H. Wang, Q. Xue, W. Peng and Q. Zhou, *J. Ethnopharmacol.*, **346**, 119636 (2025); https://doi.org/10.1016/j.jep.2025.119636
4. E. Duranti, N. Cordani and C. Villa, *Int. J. Mol. Sci.*, **25**, 1633 (2024); https://doi.org/10.3390/ijms25031633
5. F. Bray, M. Laversanne, H. Sung, J. Ferlay, I. Soerjomataram, R.L. Siegel, and A. Jemal, *CA Cancer J. Clin.*, **74**, 229 (2024); https://doi.org/10.3322/caac.21834
6. J. Kuzminska, P. Szyk, D.T. Mlynarczyk, P. Bakun, I. Muszalska-Kolos, K. Dettlaff, A. Sobczak, T. Goslinski and A. Jelinska, *Molecules*, **29**, 5321 (2024); https://doi.org/10.3390/molecules29225321
7. C. Salami, J.P. Mbakidi, S. Audonnet, S. Brassart-Pasco and S. Bouquillon, *Molecules*, **30**, 1180 (2025); https://doi.org/10.3390/molecules30051180
8. U.A. Rahim, M. Mustapa, N.N.S.M. Shakrin, A. Nurdin, N.M. Taridi, Y.A.M. Yusof, M.F. Mad Nordin and N.A. Che Roos, *PLoS One*, **19**, e0314280 (2024); https://doi.org/10.1371/journal.pone.0314280
9. P. Goleij, A. Rezaee, H.Y. Lam, M.A.K. Tabari, D. Alijanzadeh, N. Ouf, P.M. Sanaye, D.S. Larsen, M. Daglia, H. Khan, G. Sethi and A.P. Kumar, *Inflammopharmacology*, **33**, 2293 (2025); https://doi.org/10.1007/s10787-025-01739-5
10. D. Khayatan, S.M. Razavi, Z.N. Arab, H. Nasoori, A. Fouladi, A.V.K. Pasha, A.E. Butler, S. Karav, S. Momtaz, A.H. Abdolghaffari and A. Sahebkar, *Inflammopharmacology*, **33**, 1583 (2025); https://doi.org/10.1007/s10787-025-01643-y
11. M.R. Islam, A. Rauf, S. Akter, H. Akter, M.I.K. Al-Imran, M.N.H. Fakir, G.K. Thufa, M.T. Islam, H.A. Hemeg, W.A. Abdulmonem, A.S.M. Aljohani and M. Iriti, *J. Biochem. Mol. Toxicol.*, **39**, e70369 (2025); https://doi.org/10.1002/jbt.70369
12. Y. Yuan, H. Huang, T. Hu, C. Zou, Y. Qiao, M. Fang, J. Liu and S. Lai, *Int. J. Mol. Med.*, **54**, 110 (2024); https://doi.org/10.3892/ijmm.2024.5434
13. M. Roney, A. Dubey, A.R. Issahaku, M.N. Uddin, A. Tufail, A. Wilhelm, N.B. Zamri and M.F.F.M. Aluwi, *J. Biomol. Struct. Dyn.*, **43**, 4942 (2025); https://doi.org/10.1080/07391102.2024.2306197
14. H. Gu, S. Liu, K. Liang, Z. Xia, G. Zhang, B. Li and S. Liu, *Molecules*, **29**, 1985 (2024); https://doi.org/10.3390/molecules29091985
15. P. Bakun, M. Wysocki, M. Stachowiak, J. Dlugaszewska, M. Musielak, D.T. Mlynarczyk, L. Sobotta, W.M. Suchorska and T. Goslinski, *Molecules*, **29**, 4536 (2024); https://doi.org/10.3390/molecules29194536
16. Y. González, R. Mojica-Flores, D. Moreno-Labrador, L. Cubilla-Rios, K.S.J. Rao, P.L. Fernández, O.V. Larionov and J. Lakey-Beitia, *Int. J. Mol. Sci.*, **24**, 3691 (2023); https://doi.org/10.3390/ijms24043691
17. X.Y. Zhao, J.Y. Lu, L. Zheng, M. Yan, S.H. Zhang, S. Chen, Q. Zhang, X. Jiang, Y. Tan, T.F. Li and F. Leng, *Int. J. Biol. Macromol.*, **314**, 144291 (2025); https://doi.org/10.1016/j.ijbiomac.2025.144291
18. H. Alici, *Pharmaceuticals*, **18**, 798 (2025); https://doi.org/10.3390/ph18060798
19. Y. Zhou, J. Gong, X. Deng, L. Shen, S. Wu, H. Fan and L. Liu, *Biomed. Pharmacother.*, **180**, 117404 (2024); https://doi.org/10.1016/j.biopha.2024.117404

20. B. Mayo, S. Penroz, K. Torres and L. Simón, *Int. J. Mol. Sci.*, **25**, 11492 (2024); https://doi.org/10.3390/ijms252111492
21. L.C. Gutsche, J. Dörfler and J. Hübner, *Eur. J. Clin. Pharmacol.*, **81**, 1 (2025); https://doi.org/10.1007/s00228-024-03764-9
22. M. Sichetti, M. Giuseffi, E. Giglio, G. Marino and M. Mecca, *Mol. Nutr. Food Res.*, **69**, e70055 (2025); https://doi.org/10.1002/mnfr.70055
23. M. Duan, A. Mahal, A. Alkouri, C. Wang, Z. Zhang, J. Ren and A.J. Obaidullah, *Molecules*, **29**, 3010 (2024); https://doi.org/10.3390/molecules29133010
24. M.J. Zhang, M. Shi, Y. Yu, R. Ou, R.S. Ge and P. Duan, *Mol. Carcinog.*, **63**, 1449 (2024); https://doi.org/10.1002/mc.23735
25. N.F.C. Rahim, Y. Hussin, M.N.M. Aziz, M.J. Masarudin, S.A. Gani, M.N. Akhtar, N.M.A.N. Abd. Rahman and N.B. Alitheen, *Anticancer. Agents Med. Chem.*, **25**, 774 (2025); https://doi.org/10.2174/0118715206336788241029050155
26. S. Goenka, F. Johnson and S.R. Simon, *Biomolecules*, **11**, 674 (2021); https://doi.org/10.3390/biom11050674
27. W. Cao, P. Yu, Y. Cao, S. Feng and N. Yin, *Sci. Rep.*, **15**, 8181 (2025); https://doi.org/10.1038/s41598-025-93451-1
28. A.S.A. Yassen, S.M. Abdel-Wahab, K.M. Darwish, M.S. Nafie, R.F.A. Abdelhameed, G.S. El-Sayyad, A.I. El-Batal, K.M. Attia, H.A. Elshihawy and R. Elrayess, *RSC Med. Chem.*, **15**, 4039 (2024); https://doi.org/10.1039/D4MD00574K
29. R. Murwanti, Ritmaleni, N.S.O. Ujiantari, I.M.R. Putra, A.F. Wahyudi and V.I. Arifka, *Curr. Res. Toxicol.*, **8**, 100230 (2025); https://doi.org/10.1016/j.crtox.2025.100230
30. H. Wahnou, R. El Kebbaj, B. Liagre, V. Sol, Y. Limami and R.E. Duval, *Pharmaceutics*, **17**, 114 (2025); https://doi.org/10.3390/pharmaceutics17010114
31. B. Rathnakar, G.S. Kumar, S.P. Mahammad, S. Gattu, S. Kalyani, R. Nimma and M. Satyanarayana, *J. Heterocycl. Chem.*, **58**, 488 (2021); https://doi.org/10.1002/jhet.4186
32. V. Sudarshan, P. Shyamjith, S. Kumar, F. Ravindran, B. Choudhary and S.S. Karki, *Int. J. Mol. Sci.*, **26**, 3186 (2025); https://doi.org/10.3390/ijms26073186
33. F.C. Rodrigues, N.V.A. Kumar and G. Thakur, *Pharmacol. Res.*, **166**, 105489 (2021); https://doi.org/10.1016/j.phrs.2021.105489
34. Y. Yin, Y. Tan, X. Wei, X. Li, H. Chen, Z. Yang, G. Tang, X. Yao, P. Mi and X. Zheng, *Chem. Biodivers.*, **19**, e202200485 (2022); https://doi.org/10.1002/cbdv.202200485
35. H. Dai, S. Zhang, X. Zheng, Z. Luo, H. Chen and X. Yao, *Chem. Biodivers.*, **21**, e202301556 (2024); https://doi.org/10.1002/cbdv.202301556
36. G. Feriotto, R. Rondanin, P. Marchetti, F. Tagliati, S. Beninati, C. Tabolacci, E. Grusi, S. Aguzzi and C. Mischiati, *Life*, **13**, 431 (2023); https://doi.org/10.3390/life13020431
37. W.H. Lee, C.Y. Loo, M. Bebawy, F. Luk, R.S. Mason and R. Rohanizadeh, *Curr. Neuropharmacol.*, **11**, 338 (2013); https://doi.org/10.2174/1570159X11311040002
38. A. Daina, O. Michielin and V. Zoete, *Nucleic Acids Res.*, **47**, 357 (2019); https://doi.org/10.1093/nar/gkz382
39. S. Sogabe, Y. Kawakita, S. Igaki, H. Iwata, H. Miki, D.R. Cary, T. Takagi, S. Takagi, Y. Ohta and T. Ishikawa, *ACS Med. Chem. Lett.*, **4**, 201 (2013); https://doi.org/10.1021/ml300327z